Mean Flow Measurements in Turbulent Boundary Layers along Mildly Curved Surfaces

B.R. Ramaprian*
Iowa State University, Ames, Iowa
and
B.G. Shivaprasad†
Indian Institute of Science, Bangalore, India

An experimental investigation of the mean flow characteristics of two-dimensional turbulent boundary layers over surfaces of mild longitudinal curvature is reported. The study covered both convex and concave walls of $|\delta/R_w| \approx 0.013$ (δ being the boundary-layer thickness and R_w being the wall radius). It was found that, whereas the region close to the wall was not affected significantly by wall curvature, the outer region was very sensitive to even mild wall curvature. A detailed study of the wake region using present and other available data suggests a systematic effect of δ/R_w on the wake structure. The paper also discusses in detail the effect of mild wall curvature on the boundary-layer development with particular emphasis on the difference in behavior of the boundary layer at short and long distances from the leading edge of the curved wall, an aspect which has not received sufficient attention in previous experimental investigations. An attempt has been made to explain this behavior from a consideration of the structure of turbulence in boundary layers over curved surfaces.

I. Introduction

THERE are many engineering applications where turbulent boundary layers over longitudinally curved surfaces are encountered. Some examples are blade passages of turbomachinery, wings and intakes of aircraft, hubs of propellers, and rocket nozzles. Traditionally, such boundary layers have been calculated by ignoring wall curvature and using turbulent models appropriate to flat-wall boundary layers. However, Bradshaw[1] showed that the behavior of the turbulent boundary layer is very sensitive to streamline curvature and that even a very mild wall curvature (corresponding to $|\delta/R_w| = 1/300$, where δ is the boundary-layer thickness and R_w is the wall radius taken to be positive for convex curvature and negative for concave curvature) can cause a significant effect on the structure of turbulence in the boundary layer. Other analytical and experimental studies generally have confirmed Bradshaw's observations.

Although it was Bradshaw's work which focused attention on the effects of wall curvature, there were also some earlier studies of curvature effects on turbulent boundary layers and turbulent channel flows.[2-7] Also, the experiments of Schubauer and Klebanoff[8] over a wing surface can be added to this list though their experiments were not directed primarily toward investigating curvature effects. In the paper referred to earlier, Bradshaw used the concept of analogy between the effects of streamline curvature and buoyancy (an idea originally suggested by Prandtl[9]) to estimate quantitatively the effect of curvature on the mixing length distribution in the boundary layer from information available on the effect of buoyancy on the mixing length distribution in the atmospheric boundary layer. After Bradshaw's[1] paper appeared, interest grew rapidly in this area and a number of studies have been reported in the past few years. These include both experimental investigations[10-16] and analytical/computational efforts.[17-22] A very comprehensive survey of the literature on curvature effects is available from a review article by Bradshaw.[15]

With the exception of the work of Ellis and Joubert[13] and Meroney,[14] much of the available experimental data relate to flows over strongly curved surfaces ($|\delta/R_w| \gtrsim 0.04$). In fact, at the time the present work was started, there were hardly enough data available to make a direct verification of Bradshaw's predictions of the effects of mild curvature. In view of this and also in view of the practical importance of the study (e.g., in such problems as flow over aerofoils), the authors undertook an extensive experimental study of the effect of mild wall curvature ($\delta/R_w \approx \pm 0.013$) on the behavior of the turbulent boundary layer. The investigation covered the study of curvature effects on both the mean and turbulent characteristics of the flow and is reported in detail in Ref. 23. The present paper reports mainly the results pertaining to curvature effects on the behavior of the mean flow. The present experiments corroborated the observations of other investigators in many respects; but also revealed some interesting and significant deviations. The paper makes a careful examination of the structure of the mean velocity distributions and the development of the boundary layer over the curved wall, in the light of these new experimental observations.

II. Experimental Program

A. Experimental Scheme

The experimental program consisted of the measurement of flow quantities in boundary layers developing over convex and concave walls. Although $|\delta/R_w|$ varied along the test section, its average value was about 0.013. The experiments were designed in such a way as to study the effects of curvature by isolating them, as far as possible, from other influences such as longitudinal pressure gradient and secondary flow. It was verified that the boundary layer had the structure of a fully developed, zero pressure gradient flat-wall boundary layer before approaching the curved wall.

B. Experimental Apparatus

Figure 1 shows the layout of the experimental apparatus used. Air from the 2-hp centrifugal blower passed through a diffuser, a settling chamber, and a two-dimensional con-

Received May 5, 1976; revision received Aug. 20, 1976.
Index category: Boundary Layers and Convective Heat Transfer—Turbulent.

*Visiting Assistant Professor, Department of Mechanical Engineering and Engineering Research Institute. Currently Research Engineer, Iowa Institute of Hydraulic Research, University of Iowa, Iowa City, Iowa.
†Project Assistant, Aeronautical Engineering Dept.

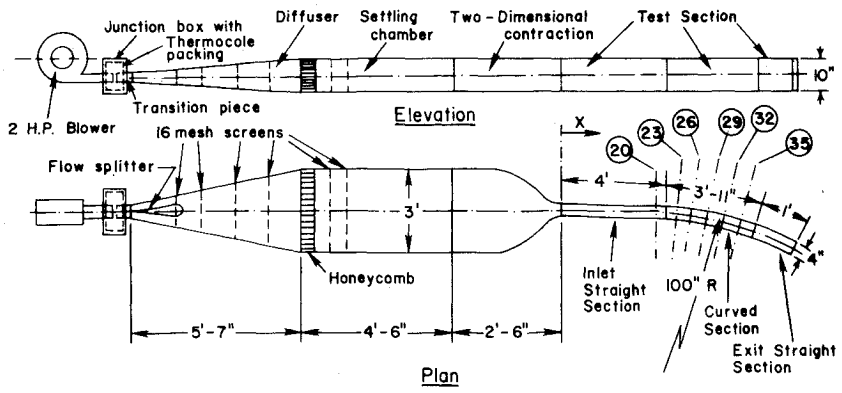

Station No.		20	23	26	29	32	35
X (in)	Convex wall	40.6	50.5	59.3	68.2	77.0	85.8
	Concave wall	40.6	50.8	59.9	69.1	78.3	87.5

Not to Scale

Fig. 1 Layout of the experimental apparatus.

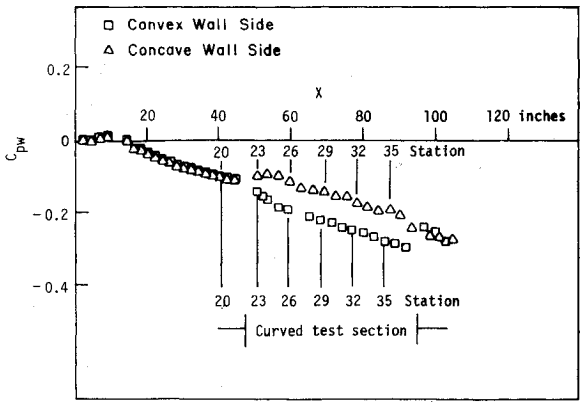

Fig. 2 Static pressure distribution along the two walls of the test section.

traction of area ratio 9:1, before entering the test section. The thermocole junction served to absorb the vibrations and significantly reduce the noise and freestream turbulence level at the test section. The test section consisted of an initial straight duct 1-ft long, a curved duct approximately 4-ft long and, an exit straight duct 1-ft in length. The initial straight section was used for getting a fully developed, zero pressure gradient turbulent boundary layer at inlet to the test section. The 1-ft exit section served to prevent ambient air currents from affecting the flow in the curved section. The ducts had a rectangular cross section of 10×4 in. The 10-in. sidewalls were made of Plexiglas and were used as the test surfaces. The sidewalls of the curved duct were concentric circles of radii 98 in. and 102 in. and were used, respectively, as the convex and concave surfaces on which the turbulent boundary layers were studied. It was insured from preliminary experiments that the boundary layers over the convex and concave walls were separated from each other by an inviscid "nonturbulent" core region of at least about 0.75 in. even at the end of the curved duct. The measurement stations were located at midheight of the test section at 9-in. intervals. The location of the measurement stations along the test sections and their designations also are shown in Fig. 1. Static pressure holes of 0.040 in. diameter were provided on the side walls at 3-in. intervals at heights of 2.5, 5, and 7.5 in. from the bottom wall.

In view of the rather small aspect ratio of the test section, special care was taken to check and insure that there was no significant secondary flow at least in the vicinity of the measurement stations. For this purpose, three independent checks were made, viz. a yaw probe transverse across the test section, an integral momentum balance check and a measurement of the distribution of the Reynolds stress component $\overline{\rho uw}$ across the test section. These checks indicated that although secondary flow indeed was present over a large part of the test section, it was insiginficant up to a distance of 1 in. above and below the plane of measurement. Detailed results of these checks are reported in Ref. 23.

The longitudinal wall static pressure (p_w) distribution was measured on both walls using the wall static taps. The total head (p_t) distribution across the boundary layers over the two walls was measured by traversing a round total head tube of 0.032-in. diameter in the radial direction. The same tube was used as a Preston tube for measuring the wall-shear stress τ_w. The distribution of the static pressure p in the radial direction was measured in some cases (stations 23 and 26) by traversing a disk probe of ⅜-in. diameter. For stations 29 to 35, it was found to be adequate to determine p from the total head readings by using the radial momentum equation (see for example Eskinazi and Yeh[3])

$$\frac{\partial p}{\partial R}=\frac{\rho\bar{U}^2}{R}=\frac{2(p_t-p)}{R} \qquad \text{(neglecting turbulence terms)} \quad (1)$$

or

$$p=p_{wx}+\int_{R=R_{wx}}^{R}2(p_t-p)\frac{dR}{R} \qquad (2)$$

where R is the streamline radius at any point and the subscript wx refers to the value on the convex wall. The mean velocity $\bar{U}$ at any point was obtained from the local values of p_t and p.

III. Results

A. Longitudinal Pressure Distribution

The longitudinal static pressure distribution was measured on both walls of the test section at midspan as well as other spanwise positions. No significant difference in wall static pressure was observed in the spanwise direction. Hence, only the pressure distribution at midheight position is presented in Fig. 2. In this figure, the wall static pressure is plotted in terms of a nondimensional pressure coefficient C_{pw} defined as

$$C_{pw}=(p_w-p_{cw})/\tfrac{1}{2}\rho(\bar{U}_\infty)_{20}^2 \qquad (3)$$

where p_{cw} is the reference wall static pressure at the contraction exit and $(\bar{U}_\infty)_{20}$ is the reference velocity at the centerline of Station 20.

In order to keep the design simple, the area of cross section of the test section was not varied to accommodate the growth of boundary layers along the walls. This resulted in an overall

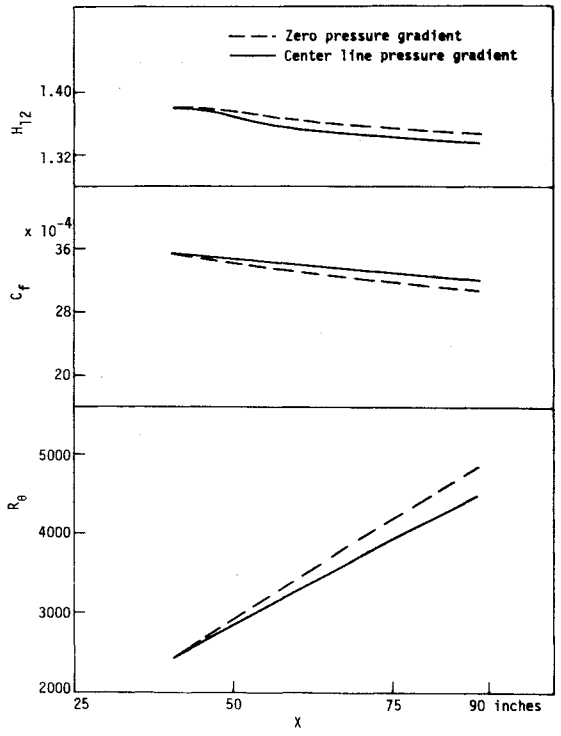

Fig. 3 Predicted development of boundary-layer parameters over a flat wall, using the method of Rotta.[24]

"mild" favorable pressure gradient along the test section instead of the more desirable zero pressure gradient. This can be seen from Fig. 2. In order to isolate the effect of curvature from any effect of this "mild" pressure gradient, calculations were made to estimate the development of the boundary layer over a flat wall under the actual pressure gradient existing in the tunnel. These calculations were made using the shear work integral method of Rotta.[24] This method was used as it was found to have given satisfactory results for mild favorable pressure gradients. A computer program was written for this purpose on the exact lines outlined in Ref. 24. Figure 3 shows the computed development of the momentum thickness Reynolds number R_θ, the skin friction coefficient C_f, and the shape factor H_{12} along a flat plate under two conditions: 1) zero pressure gradient (dashed lines) and 2) pressure gradient existing along the centerline of the test section (full lines). The skin friction coefficient is defined as $\tau_w/\frac{1}{2}\rho\bar{U}_{pw}^2$, where $\bar{U}_{pw}$ is the potential velocity on the wall equal to Ω/R_w and Ω is the angular momentum in the freestream. The initial conditions in both the cases correspond to those at station 20 on the flat wall. From the figure it is seen that the effect of the favorable pressure gradient is to reduce slightly R_θ and H_{12} and increase slightly the values of C_f. The full lines rather than the dashed lines therefore will be used to compare with the experimental data. It will be assumed that this procedure is sufficient to isolate the curvature effect.

The second observation that can be made from Fig. 2 is the presence of kinks in the pressure distribution curve at the beginning and end of curvature. These kinks are a result of the adjustment of the flow from the zero pressure gradient prevailing across the straight section to the radial pressure gradient existing in the curved section. It is observed as a favorable pressure gradient at the beginning of the convex wall and an adverse pressure gradient at the beginning of the concave wall. The opposite situation is observed at the end of the curved test section. (It was insured by flow visualization using tufts that the adverse pressure gradients did not cause flow separation.) These sudden changes in the pressure distribution, however, are seen to die out within a short distance. Over most of the curved section, such as from station 25 to station 36 (i.e. over a distance of about 3 ft in the middle) the pressure gradient is almost constant and is about the same for both the walls.

B. Mean Velocity Profiles in the Inner Coordinates

Figure 4 shows the mean velocity profiles on convex and concave walls plotted in the inner layer coordinates. It can be seen that near the wall the experimental data for both convex and concave walls agree with the same log law; $u^+ = 5.6 \log y^+ + 5.5$, as observed in the case of the flat wall at station 20. However, the range of this log region is $25 < y^+ < 250$ for the convex wall, whereas it is $25 < y^+ < 700$ in the case of the concave wall. These observations are in general conformity with the findings of Patel[7] ($\delta/R_w \approx \pm 0.06$) and Ellis and Joubert[13] ($\delta/R_w \approx 0.044$, 0.013). The observations of So and Mellor[11] in the case of strong convex curvature ($\delta/R_w \approx 0.1$) are also in agreement with the present results. However, their study[12] indicated a reduced log law region even with strong concave wall curvature ($\delta/R_w \approx -0.1$). In any case, the present data allow us to conclude that the midly curved convex and concave surfaces the inner layer behaves in the same way as a flat-plate boundary layer.

Contrary to the inner layer behavior, the outer layer shows a departure from the normal flat-plate boundary-layer profiles. Over the convex wall, the departure from the log law initially decreases as at station 23 due to the favorable pressure gradient existing near the joint. Afterwards, however, it continuously increases as in the case of a boun-

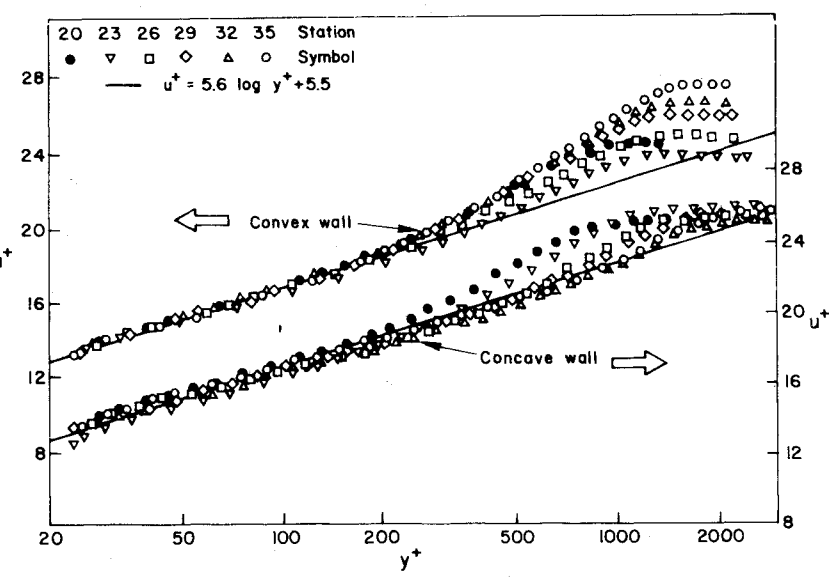

Fig. 4 Mean velocity profiles over the curved walls in wall coordinates.

dary layer subjected to an adverse pressure gradient. Over the concave wall, the opposite of this happens. The departure increases at station 23 due to an adverse pressure gradient at the joint but continuously decreases thereafter as in the case of a boundary layer subjected to a favorable pressure gradient. These trends are again in conformity with the observations of So and Mellor.[10] However, the interesting observation is that the deviation from the flat-plate behavior is quite significant, even with mild curvature. This is especially so with the boundary layer on the convex wall.

C. Mean Velocity Profiles in the Outer Coordinates

Figure 5 shows the velocity defect profiles plotted in the outer coordinates as $(\bar{U}_p - \bar{U})/u_*$ vs y/Δ, where $\bar{U}_p$ is the local potential velocity equal to Ω/R and Δ is the "Clauser-thickness," defined by

$$\Delta = \int_0^\infty \frac{\bar{U}_p - \bar{U}}{u_*} \tag{4}$$

The defect profiles for the convex wall show that the flow has not really reached an equilibrium state. From the data for stations 32 and 35, it can be said that Reynolds number similarity is exhibited only for $y/\Delta > 0.07$. The profiles exhibit semilogarithmic distributions at smaller values of y/Δ but the extent of this semilogarithmic region decreases along the wall. Where the semilogarithmic distribution exists, the slope of the log line is -5.6 at all stations (same in magnitude as that of the slope of the log line of Fig. 4). However, the intercepts are different, decreasing first at station 23 due to the sudden favorable pressure gradient and subsequently increasing progressively. Even at station 35, one does not observe any tendency of the profiles to approach a self-preserving form over the entire turbulent region. This observation is apparently in variance with the results of So and Mellor, which appear to suggest that the mean velocity profiles approached a self-preserving form towards the end of the test section. A close examination of their work, however, indicates that the successive profiles were measured at stations only 2 in. apart whereas, in the present case, the stations are 9 in. apart. It is therefore possible that in the former case the departure from equilibrium could not have been very conspicuous in the data. Alternatively, the difference between the two results may be due to the difference in the severity of curvature.

The data for the concave wall, on the other hand, present a different picture. With the exception of the profile at station 23 (a result of the sudden adverse pressure gradient) the profiles appear to settle down quickly to a nearly self-preserving form. Again, at small values of y/Δ, a semilogarithmic distribution with a slope of -5.6 can be observed. The intercepts decrease from station to station but the decrease is very small. The entire profile seems to have attained approximate self-preservation by the time the flow reaches station 35.

Figure 6 shows a comparison, in defect coordinates, of the velocity profiles over convex and concave walls at station 35. Only the part of the profiles for $y/\Delta > 0.07$ is relevant for comparison, as this part alone represents the self-similar profile for the convex wall. A clear difference can be observed in the velocity profiles over the two walls. This comparison shows that even mild curvature has a very significant effect on the mean flow structure of the turbulent boundary layer.

D. Structure of the Wake

It was mentioned that the velocity profile in the outer layer is strongly affected by wall curvature. The effect on the outer layer can be understood better by describing the velocity distribution in terms of the well-known Coles log plus wake profile,[25]

$$\bar{U}/u_* = \{5.6 \log(yu_*/\nu) + 5.5\} + (\pi/\kappa) W(y/\delta_w) \tag{5}$$

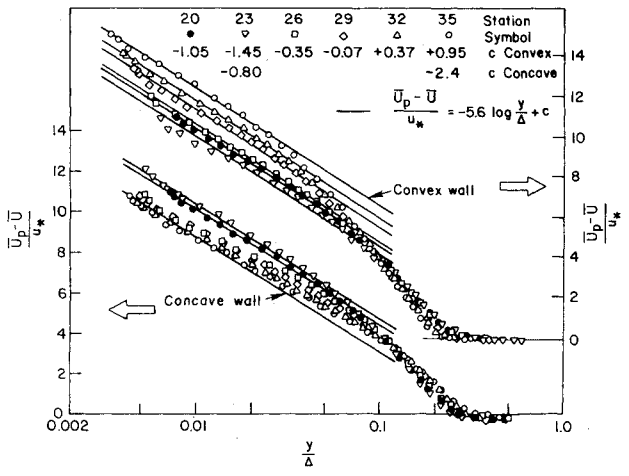

Fig. 5 Mean velocity profiles over the curved walls in outer coordinates.

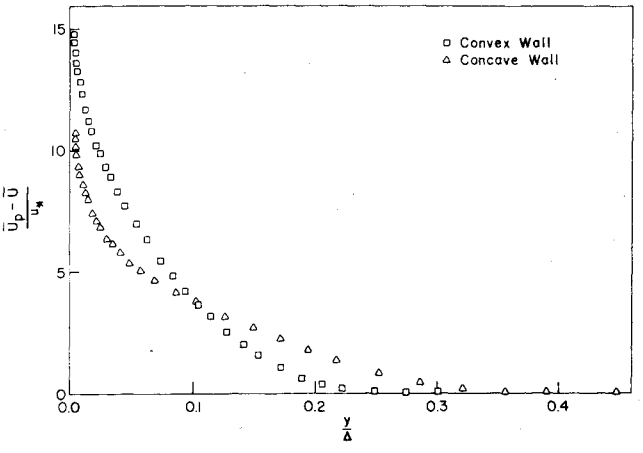

Fig. 6 Comparison of the defect profiles of velocity over convex and concave walls at station 35.

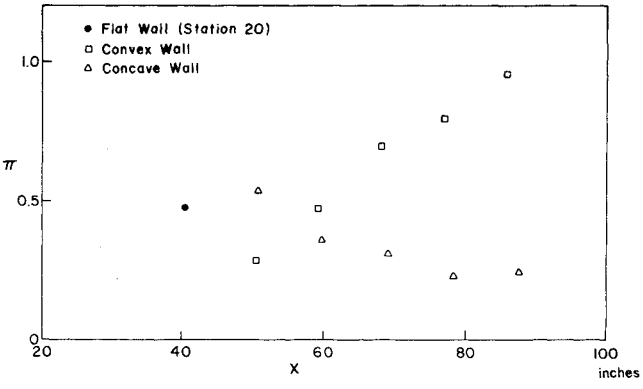

Fig. 7 Comparison of the distribution of π along convex and concave walls.

where δ_w is the distance from the wall at which the departure $(\Delta\bar{U}/u_*)$ of the velocity profile from the log law reaches the maximum value (see Fig. 4) and κ is the Karman constant assumed to be 0.4. The universal wake function of Coles W, often is described by the polynomial

$$W = 2[3(y/\delta_w)^2 - 2(y/\delta_w)^3] \tag{6}$$

The wake strength parameter π is a function of R_θ in general, but is constant for an equilibrium boundary layer. For a flat-plate boundary layer the value of π varies only from 0.47–0.5

in the range of Reynolds number encountered in the present experiments. Figure 7 shows the variation of π over the curved walls. On the convex wall, it first drops at station 23 but then increases continuously to a value of about 0.93 at station 35. In fact, it does not show any trend of settling down even at station 35. The behavior of π resembles that which is observed in adverse pressure gradient flows on flat walls. In contrast with this, the value of π decreases gradually along the concave wall (after an initial rise at station 23) until it appears to settle down to an equilibrium value around 0.25 beyond station 32. This trend qualitatively resembles that observed in favorable pressure gradient flows on flat walls. These observations are consistent with experimental results of other investigators.

In fact, these observations lead some of the investigators (Eskinazi and Yeh,[3] Patel[7]) to regard the effect of wall curvature to be equivalent to that of the longitudinal pressure gradient of appropriate sign. The limitation of the scope of this analogy can be seen from Fig. 6. It is observed that although the wall shear stress over the convex wall is less than that over the concave wall (see Figs. 10 and 11), the velocity profile over the concave wall appears to exhibit a point of inflection whereas the velocity profile over the convex wall does not. This behavior is observed even more clearly from the data from strongly curved walls (see for example So and Mellor[10]). It is particularly interesting that the velocity profile over the convex wall with the stronger wake does not show any point of inflection normally associated with an adverse pressure gradient profile whereas the velocity profile over the concave wall with a weak wake exhibits a point of inflection. It is thus clear that the analogy with longitudinal pressure gradient is applicable only to the limited extent.

A further evidence of this limitation is provided by a detailed study of the wake function W. Figure 8 shows the wake functions for the convex and concave walls as defined by Eq. (5). The full line is the universal wake function of Coles given by Eq. (6). The present flat-plate data at station 20 nearly agree with the universal profile. The figures indicate that the wake functions for the curved walls are different from the universal wake function of Coles. When compared with the flat wall, the wake defects are higher for the convex wall. The wake functions for the convex wall exhibit near self-similar behavior (except that for station 23 which corresponds to the first station of measurement). The data for the concave wall also exhibit a self-similar behavior but with the exception of the data for station 32. Owing to the small values of the wake defects on the concave wall, these values are uncertain to some extent. The deviation of these data at station 32 from the general trend cannot be explained in any other way at this stage.

The wake functions obtained from the present convex and concave wall data are compared in Fig. 9 with the wake functions computed from the data available from the experiments of So and Mellor ($\delta/R_w \approx 0.1$, $dp/dx=0$, and $dp/dx>0$), and Ellis and Joubert ($\delta/R_w \approx 0.067$, $dp/dx=0$). The comparison is based on very limited data but it appears to indicate that the wake function depends on δ/R_w and is almost independent of the longitudinal pressure gradient. Another significant observation that can be made is that the departure of the wake function from the universal wake function of Coles seems to be a nonlinear function of δ/R_w. In other words, the departure is relatively very large with mild wall curvature of either sign and stronger wall curvature does not produce a proportionately larger departure. These conclusions are to be treated as tentative at present. A more definite and quantitative description of the behavior of the wake function will be possible when more information on velocity profiles as a function of δ/R_w, pressure gradient, and Reynolds number becomes available. In fact, the usefulness of a log plus wake type of profile itself requires re-examination especially for boundary layers over strongly curved concave surfaces, in which case, the maximum wake defect itself is negative. (This, indeed, is the case with the concave wall data of So and Mellor.[12]) It may be worthwhile to investigate a three-layer model for describing the velocity profile, with the conventional log and wake regions being separated by a middle layer which is affected significantly by curvature. Some effort in this direction has been made by So and Mellor.[10] There is still need for further work in this area.

E. Boundary-Layer Development Over the Curved Walls

The variations of the momentum thickness Reynolds number R_θ, skin friction coefficient C_f, *and shape factor* H_{12} with longitidinal distance are shown in Figs. 10 and 11 for the two walls. The experimental results are compared with the

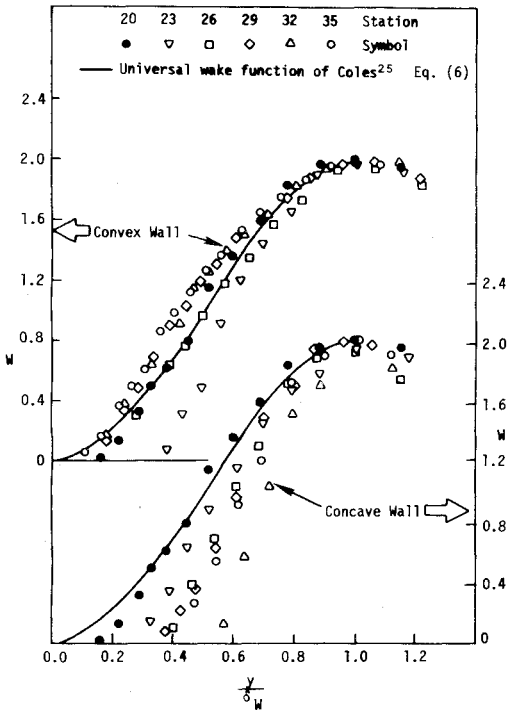

Fig. 8 Wake functions for the curved walls.

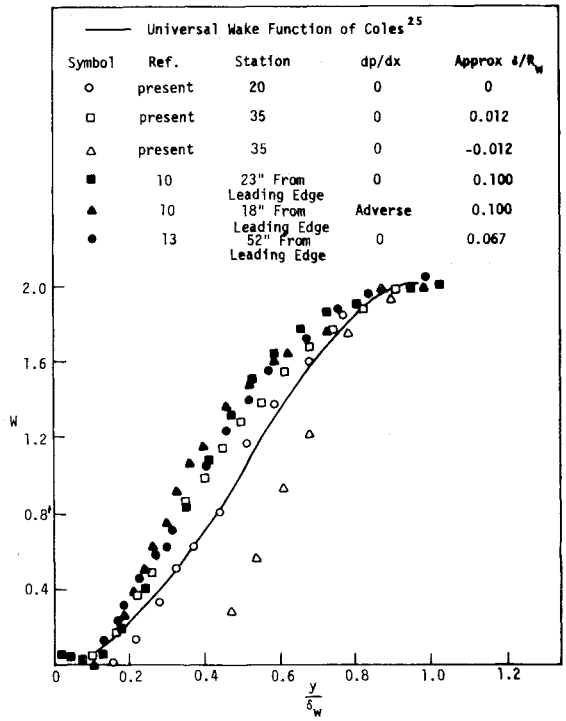

Fig. 9 Dependence of wake function on curvature.

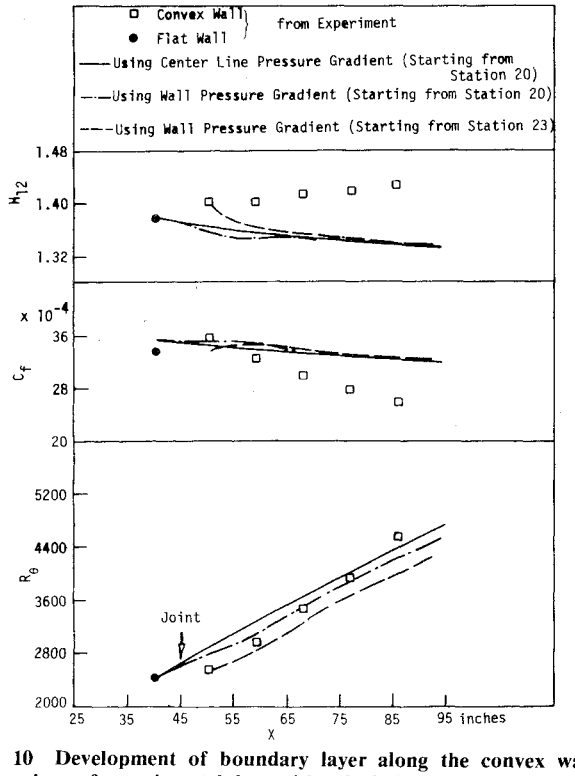

Fig. 10 Development of boundary layer along the convex wall: comparison of experimental data with calculations using the method of Rotta.[24]

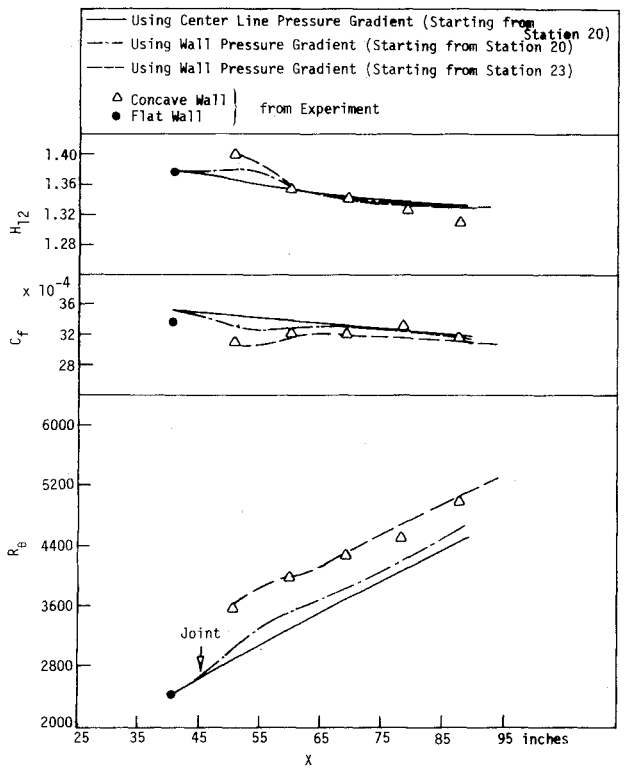

Fig. 11 Development of boundary layer along the concave wall: comparison of experimental data with calculations using the method of Rotta.[24]

predictions obtained from Rotta's[24] method for flat walls. The full lines in each figure represent the predictions obtained by assuming the longitudinal pressure gradient to be the same as the pressure gradient existing along the centerline of the test section. These are the same as the full lines in Fig. 3. The chain dotted line is obtained by using the pressure gradient along the particular wall. Both of these predictions are obtained by using the measured values of R_θ and H_{12} on the flat wall at station 20 as the initial conditions. The total effect of curvature on the boundary-layer development is represented by the deviation of the experimental data from the full line.

Previous investigators who studied the effects of longitudinal curvature on boundary-layer growth observed that the boundary layer grew at a larger rate over the concave wall whereas the rate of growth was suppressed on the convex wall. It is somewhat paradoxical that the concave wall boundary layer with a velocity profile having a weak wake grows faster, whereas even with a strong wake the boundary layer over the convex wall grows slower. It will be interesting to examine the present results in the above light. Considering first the convex wall, one can see from Fig. 10 that, as soon as the curvature starts, the rate of growth of R_θ falls, but beyond about 10 in. from the joint the rate of growth actually increases to a value larger than that for the flat plate. Toward the end of the test section, the measured values of R_θ are, in fact, slightly more than that predicted by flat-plate calculations. However, the value of R_θ is still less than that for the flat plate even at 30 in. from the joint. The skin friction coefficient, after an initial increase up to station 23, shows a continuously decreasing trend and is, in fact, lower than the predicted value for flat wall everywhere beyond an initial distance of 10 in. from the joint. The shape factor is everywhere higher than that for the flat wall. The present data of R_θ at large distances from the joint may, at first sight, appear to contradict the observations of previous investigators, e.g., So and Mellor.[10] However, a careful examination of their data discloses that the distance of the last station (from the joint) at which R_θ was measured was only about 23 in. and that most of the large decrease in R_θ occurred at the beginning of curvature itself. In fact, their data for the last two stations did exhibit a trend towards increased rate of growth relative to the flat plate. The experimental data of these authors for separating flow on a convex wall also showed slightly larger growth rates for R_θ than that predicted for zero curvature. The calculations of Eide and Johnston[16] also indicate a small increase in growth rate of R_θ with curvature.

It appears to be conceptually advantageous to divide the total effect of curvature on boundary-layer development into three constituents: 1) the effect of change in curvature or what one might call a "dR_w/dx effect," 2) the effect of local pressure gradient along the wall brought into existence by the change in the radial pressure gradient from zero on the flat wall to a nonzero value over the curved wall, and 3) the effect of sustained wall curvature or what one might call an "R_w effect."

It is rather difficult to isolate these effects. At short distances, all three effects may be important. The data however tend to show that 1 and 2 have a dominant effect in this region. Some estimate of the pressure gradient effect can be made by comparing the predictions represented by the full lines and chain dotted lines in Fig. 10. It is seen that the pressure gradient effect is not large and also that the boundary layer nearly recovers from the pressure gradient effect by about station 26. The result obtained from calculation is strictly valid for flat wall flow; but can be assumed to be not unrealistic for the curved wall also. With such an assumption, the deviation of the experimental data from the chain dotted curve represents the sum of effects 1 and 3. The "dR_w/dx effect" is seen to dominate over the "R_w effect" at short distances from the joint. At large distances from the joint, the "R_w effect" is the dominant one with the "dR_w/dn effect" affecting the growth only through the initial conditions. The effect of these initial conditions on the further development of boundary layer over a flat wall can be seen from the dashed lines in Fig. 10. These lines represent the predictions obtained by assuming the pressure gradient to be the same as the wall

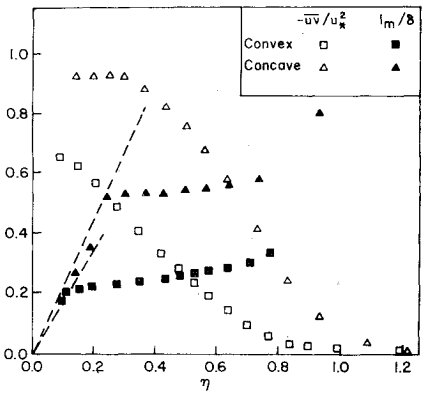

Fig. 12 The distribution of the Reynolds shear stress and mixing length over the curved walls at station 35.

pressure gradient, but using the conditions at station 23 as the initial conditions. The predictions represented by the dashed lines are seen to approach quickly those represented by the chain dotted or full lines with regard to C_f, H_{12}, and the rate of growth of R_θ. The difference between the dashed line and the experimental data represents approximately the "R_w effect" or the effect of sustained curvature, which causes an increased rate of growth of R_θ, lowers C_f, and increases H_{12}. It is likely that in previous experiments, the test sections were not long enough to allow the "R_w effect" to be observed.

Figure 11 shows the results for the concave wall. A very important point to be mentioned here is that neither the mean flow measurements nor the turbulent intensity measurements made at several spanwise positions could pick up the presence of any organized toroidal vortices of the Taylor-Görtler type. Some previous investigators have reported their presence in flows over concave walls (e.g. Tani,[6] So and Mellor[10,12]). Meroney's[14] data for $\delta/R_w=0.01$ also indicate the presence of the vortex and a significant variation of R_θ, C_f, and H_{12} across the vortex. In fact, his experimental data along the midspan line did not vary smoothly. In the present experiments, these properties varied smoothly with only a small scatter as can be seen from Fig. 11. It is difficult to say why the Taylor-Görtler vortices were not observed in the present experiments. One possible reason is that the presence of a significant amount of secondary flow in the test section (even though not in the vicinity of the plane of measurement) inhibited the development of these vortices.

In Fig. 11 the same prediction lines have been shown as have been discussed in connection with the convex wall. The experimental data in general exhibit a trend qualitatively opposite to that for the convex wall. The sustained effect of curvature, however, as indicated by the deviation of the experimental data from the dashed lines, is seen to be small. The observed larger values of R_θ everywhere on the concave wall are due essentially to the large rise of R_θ in the initial phase. The comments on the breakup of the total effect of curvature into three constituents and the recovery from induced pressure gradient are seen to apply equally well to both convex and concave walls.

In order to explain the difference in the nature of the boundary-layer development at short and large distances from the joint, one needs information on the structure of turbulence in the boundary layer over the curved wall. It is now well known that convex wall curvature reduces turbulent mixing whereas concave wall curvature enhances turbulent activity. The turbulence data obtained during the present investigation confirmed this. In fact, the effect of mild wall curvature on the turbulence structure was found to be much stronger than suspected. This is seen clearly from Fig. 12 which shows the typical effect of wall curvature on the distributions of the Reynolds shear stress ($\rho\overline{uv}$) and mixing length (l_m) across the boundary layers over the convex and concave walls at station 35. It is seen that compared to the flat wall boundary layer (at station 20), the nondimensional mixing length and Reynolds shear stress are considerably reduced over most of the convex wall boundary layer and increased, though less spectacularly, in the concave wall boundary layer. It also is seen that the region of linear mixing length variation as well as the region of "constant" shear stress are decreased by convex curvature and increased by concave curvature. Thus, over the convex wall, a large part of the boundary layer (larger than in a zero pressure gradient flat wall boundary layer) is characterized by free turbulence and exhibits a wakelike behavior. This accounts for the observed reduction in the extent of the log region in Fig. 4, and increase in the value of Coles' π in Fig. 7. Also, for the same reason, as the flow proceeds, the development of the zero-pressure gradient boundary layer over the convex wall superficially resembles that of a flat wall boundary layer with a strong wake component (as in the presence of an adverse pressure gradient). On the basis of the same reasoning, one also can expect that the boundary layer over a convex wall, when subjected to an adverse pressure gradient ultimately will grow more rapidly and separate earlier than predicted by a calculation procedure that does not consider streamline curvature effects on the turbulence structure. This expectation is, in fact, confirmed by the measurements of So and Mellor[10] in a convex wall boundary layer subjected to an adverse pressure gradient. An exactly parallel explanation can be offered for the development of the boundary layer over the concave wall. One expects in this case, that the boundary layer would eventually grow slower and separate later than predicted by flat wall calculations.

Conclusions

The following conclusions can be drawn from the present study:

1) Even mild curvature (i.e., with $|\delta/R_w| \simeq 0.013$) has a significant effect both on the mean flow structure and development of the turbulent boundary layer.

2) In the presence of mild wall curvature, the mean velocity distribution in the fully turbulent region close to the wall still follows the flat-plate log law:

$$u^+ = 5.6 \log y^+ + 5.5$$

However, the extent of the region where the log law is valid is reduced by convex curvature and increased by concave curvature.

3) The outer layer of the boundary layer is affected significantly by wall-curvature. Convex curvature increases the relative strength of the wake component whereas concave curvature reduces it in a manner roughly similar to the effect of adverse and favorable longitudinal pressure gradients, respectively. However, the analogy with pressure gradient is to be viewed with caution as curvature appears to cause the wake itself to deviate from the Coles' universal wake function for flat walls. The small amount of data presently available seem to indicate a systematic effect of curvature on the form of the wake function.

4) At short distances from the beginning of curvature, the momentum deficit thickness R_θ grows at a reduced rate over the convex wall and at an increased rate over the concave wall, as has been observed by previous investigators. This phase of the boundary-layer development is influenced predominantly by the induced longitudinal pressure gradient and the "dR_w/dx effect." At large distances, however, the influence of sustained wall curvature ("R_w effect") causes the rate of growth of R_θ to increase and C_f to decrease over the convex wall whereas an opposite effect is produced by concave curvature. This phase of boundary-layer development is controlled mainly by the relative strength of the wake like outer region of the boundary layer.

References

[1]Bradshaw, P., "The Analogy Between Streamline Curvature and Buoyancy in Turbulent Shear Flow," *Journal of Fluid Mechanics,* Vol. 36, 1969, pp. 177-191.

[2]Wattendorf, F.L., "A Study of the Effect of Curvature on Fully Developed Turbulent Flow," *Proceedings of the Royal Aeronautical Society,* 148A, 1935, pp. 565-598.

[3]Eskinazi, S. and Yeh, H., "An Investigation on Fully Developed Turbulent Flows in a Curved Channel," *Journal of the Aeronautical Sciences,* Vol. 23, 1956, pp. 23-34.

[4]Schmidbauer, H., "Behavior of Turbulent Boundary Layers on Curved Convex Wall," NACA TM 791, 1936.

[5]Clauser, M. and Clauser,F., "The Effect of Curvature on the Transition from Laminar to Turbulent Boundary Layer," NACA TN 613, 1937.

[6]Tani, I., "Production of Longitudinal Vortices in the Boundary Layer Along a Concave Wall," *Journal of Geophysical Research,* Vol. 67, 1962, pp. 3075-3080.

[7]Patel, V.C., "The Effects of Curvature on the Turbulent Boundary Layer," Aeronautical Research Council, London, Reports and Memoranda 3599, 1968.

[8]Schubauer, G.B. and Klebanoff, P.S., "Investigation of Separation of the Turbulent Boundary Layer," NACA Rept. 1030, 1951.

[9]Prandtl, L., "Effect of Stabilizing Forces on Turbulence," NACA TM 625; Translation of : "Vortrage aus dem Gebiete der Aerodynamik and Verwandter Gebiete," Aachen, 1929.

[10]So, R.M.C. and Mellor, G.L., "An Experimental Investigation of Turbulent Boundary Layers Along Curved Surfaces," NASA CR 1940, 1972.

[11]So, R.M.C. and Mellor, G.L., "Experiment on Convex Curvature Effects in Turbulent Boundary Layers," *Journal of Fluid Mechanics,* Vol. 60, 1973, pp. 43-62.

[12]So, R.M.C. and Mellor, G.L., "Experiment on Turbulent Boundary Layers on a Concave Wall," *Aeronautical Quarterly,* Vol. XXVI, 1975, pp. 35-40.

[13]Ellis, L.B. and Joubert, P.N., "Turbulent Shear Flow in a Curved Duct," *Journal of Fluid Mechanics,* Vol. 62, 1974, pp. 65-84.

[14]Meroney, R.N., "Measurement of Turbulent Boundary Layer Growth Over a Longitudinally Curved Surface," Report 74-05, 1974, Dept. of Aeronautical Engineering, Imperial College, Great Britain.

[15]Bradshaw, P., *Effects of Streamline Curvature on Turbulent Flow,* AGARDograph No. 169, 1973.

[16]Eide, A.S. and Johnston, J.P., "Predicting of the Effects of Longitudinal Wall Curvature and System Rotation on Turbulent Boundary Layers," Rept. PD-19, 1974, Dept. of Mechanical Engineering, Stanford University, Calif.

[17]Rastogi, A.K. and Whitelaw, J.H., "Procedure for Predicting the Influence of Longitudinal Curvature on Boundary-Layer Flows," ASME Paper No. 71-WA/FE-37, 1971.

[18]Papailiou, K., Satta, A., and Nurzia, F., "On the Two-Dimensional Boundary Layers as They Appear on Turbomachine Blades," *Boundary Layer Effects in Turbomachines,* AGARDograph 164, J. Surugue, Ed., 1972, pp. 5-27.

[19]Cebeci, T., "Wall Curvature and Transition Effects in Turbulent Boundary Layers," *AIAA Journal,* Vol. 9, Sept. 1971, pp. 1868-70.

[20]So, R.M.C., "A Turbulence Velocity Scale for Curved Shear Flows," *Journal of Fluid Mechanics,* Vol. 70, 1975, pp. 37-57.

[21]Irwin, H.P.A.H. and Smith, A.P., "Prediction of the Effects of Longitudinal Wall Curvature and System Rotation on Turbulent Boundary Layers," Rept. PD-19, 1974, Dept. of Mechanical Engineering, Stanford University, Calif.

[22]Johnston, J.P., and Eide, S.A., "Turbulent Boundary Layers on Centrifugal Compressor Blades: Prediction of the Effects of Surface Curvature and Rotation," *ASME 21st Annual International Gas Turbine Conference and the 18th Annual Fluids Engineering Conference,* Paper No. 76-FE-20, March 1976, New Orleans, La.

[23]Shivaprasad, B.G., "An Experimental Study of the Effects of Mild Longitudinal Curvature on the Turbulent Boundary Layer," Ph.D. Thesis, 1976, Indian Institute of Science, Bangalore, India; see also Ramaprian, B.R. and Shivaprasad, B.G., Rept. 76 FM2, 1976, Aeronautical Engineering Dept., Indian Institute of Science, Bangalore, India.

[24]Rotta, J.C., "Turbulent Boundary Layer Calculations With the Integral Dissipation Methods," *Computations of Turbulent Boundary Layers,* Vol, 1, 1968, AFOSR-IFP, Stanford Conference, pp. 177-181.

[25]Coles, D.E., "The Law of the Wake in the Turbulent Boundary Layer," *Journal of Fluid Mechanics,* Vol, 1, 1956, pp. 191-226.